

A tensegrity approach to the optimal reinforcement of masonry domes and vaults through fiber-reinforced composite materials

F. Fraternali

Department of Civil Engineering, University of Salerno, 84084 Fisciano (SA), Italy

G. Carpentieri, M. Modano

Department of Structural Engineering, University of Naples Federico II, 80132 Naples, Italy

F. Fabbrocino

Department of Engineering, Pegaso University, Piazza Trieste e Trento, 48- 80132-Naples, Italy

R.E. Skelton

Department of Structural Engineering, University of California San Diego, 92093 CA, La Jolla, United States

Abstract

We present a tensegrity approach to the optimal design of strengthening techniques of masonry vaults and domes performed by application of grids of fiber reinforced composite materials to the masonry substrate. A topology optimization approach to the masonry reinforcement is formulated, on accounting for a minimal mass design strategy, different strengths in tension and compression of the material, and multiple loading conditions. We show that the proposed optimization strategy can be profitably employed to rationally design fiber-reinforced composite material reinforcements of existing or

Email addresses: f.fraternali@unisa.it (F. Fraternali), gcarpentieri@unisa.it (G. Carpentieri), modano@unina.it (M. Modano), francesco.fabbrocino@unipegaso.it (F. Fabbrocino), bobskelton@ucsd.edu (R.E. Skelton)

new masonry vaults and domes, making use of the safe theorem of limit analysis. A wide collection of numerical examples dealing with real-life masonry domes and vaults highlight the technical potential of the proposed approach, and the corresponding optimal design of grids of composite material reinforcements.

Keywords: Masonry, Tensegrity, Topology Optimization, Minimal Mass, Vaults, Domes

1. Introduction

The field of Discrete Element Modeling (DEM) of materials and structures is growing rapidly, attracting increasing attention from physicists and mechanics working in different research areas. Originally, such a computational technique was aimed at describing particle interactions in discrete systems, via force and/or torque systems (fully discrete systems, refer, e.g., to [1] and references therein). Nowadays, DEMs are also frequently used in association with continuous approximation schemes (coupled discrete-continuum models), in order to tackle scaling limitations of purely discrete models. DEMs may indeed require a large number of variables, being well suited to describe small process zones (dislocation and fracture nucleation, nanoindentation, atomic rearrangements, etc., cf. [2–7]).

In structural mechanics, a special class of DEMs is that of equivalent truss models of solids and structures, which includes Lumped Strain/Stress Models (LSM) of plates and shells [8–10]; Thrust Network Approaches (TNA) to masonry structures [11–16]; mechanical models of chains of granular materials or carbon nanotube (CNT) arrays [17, 18]; and strut and tie models of discontinuous regions in reinforced-concrete structures [19], just to name a few examples. Some convergence studies of such methods in the continuum limit are presented in [20–22] for bending plates, 2D elasticity, and CNT arrays, respectively.

Tensegrity structures are prestressable truss structures, which are obtained by connecting compressive members (bars or struts) through the use of pre-stretched tensile elements (cables or strings). Motivated by nature [23], engineers have only recently developed efficient analytical methods for exploiting tensegrity concepts in engineering design [24–26]. Form-finding of truss-like structures continues to be an active research area, due to both their easy control (geometry, size, topology and prestress control), and the

fact that tensegrity structures provide minimum mass systems under different loading conditions [27–32].

The present work deals with the topology optimization of reinforcements of masonry vaults and domes realized through meshes of Fiber Reinforced Polymers (FRP) or Fabric Reinforced Cementitious Matrix (FRCM) composites bonded to the masonry substrate. We model such structures as tensegrity networks of masonry struts and tensile elements corresponding to the FRP-/FRCM-reinforced regions of masonry. Such reinforcements are typically applied to masonry structures in the form of meshes of 1D elements [33, 34], and are aimed at carrying tensile forces that would otherwise cause cracking damage of masonry [35–39]. The proposed optimization strategy determines the minimal mass tensegrity structure connecting a given node set, under different yielding constraints on compressive (masonry) and tensile (FRP/FRCM) elements. Each node is potentially connected to all the neighbor nodes lying in a ball of prescribed radius, through compressive and tensile elements. Such a connection pattern defines a background structure that is subject to minimal mass optimization [30], assuming different limit strengths for the masonry struts (compressive elements), and the FRP/FRCM reinforcements. An optimization procedure takes the node set defining the geometry of the structure (obtained, e.g., through a laser-scanner), the material density and the compressive and tensile material strengths as input parameters. It produces a minimal mass resisting mechanism of the reinforced structure as output, which can be regarded as a lumped stress/thrust network model of the examined structure [12, 14, 15]. Under the assumption of stable plastic response of masonry in compression and reinforcements in tension, the safe theorem of the limit analysis of elastic-plastic bodies [40] ensures that the reinforced structure is safe under the examined loading conditions. It is worth noting that the *Italian Guide for the Design and Construction of Externally Bonded FRP Systems for Strengthening Existing Structures* claims what follows: ‘Simplified schemes can also be used to describe the behavior of the structure. For example, provided that tensile stresses are directly taken by the FRP system, the stress level may be determined by adopting a simplified distribution of stresses that satisfies the equilibrium conditions but not necessarily the strain compatibility’ (see [39], Sect. 5.2.1). A minimal mass resisting mechanism allows for an optimized design of FRP-/FRCM-reinforcements, preventing excessive over-strength of the reinforced structure, which may be responsible for reduced ‘cracking-adaptation’ capacity of the reinforced structure under the given loads [41].

The paper is structured as follow. Section 2 describes the proposed tensegrity model of a reinforced masonry vault or dome, which is based on an automatically generated background structure. Next, Sect. 3 formulates a minimum mass optimization of such a structure, under given yielding constraints and multiple loading conditions. The following Section 4 presents a parade of case studies dealing with the FRP-/FRCM- reinforcement of a dome (Sect.4.1), a groin vault (or cross vault), a cloister vault (or domical vault) and a barrel vault (Sect. 4.2). Concluding remarks and prospective work are illustrated in Section 5.

2. Tensegrity model of a reinforced masonry vault

Let us consider a masonry vault or dome with mean surface described by a set of n_n nodes in the 3D Euclidean space. In a given Cartesian frame $\{\mathbf{O}, \mathbf{x}, \mathbf{y}, \mathbf{z}\}$, the components (x_k, y_k, z_k) of the position vectors \mathbf{n}_k of all such nodes ($k = 1, \dots, n_n$) can be arranged into the following $3 \times n_n$ node matrix

$$\mathbf{N} = \begin{bmatrix} x_1 & \dots & x_{n_n} \\ y_1 & \dots & y_{n_n} \\ z_1 & \dots & z_{n_n} \end{bmatrix} \quad (1)$$

We now introduce a *background structure*, which is obtained by connecting each node \mathbf{n}_k with all the neighbors \mathbf{n}_j such that it results $|\mathbf{n}_k - \mathbf{n}_j| \leq r_k$ (*interacting neighbors*). Here, $|\mathbf{n}_k - \mathbf{n}_j|$ is the Euclidean distance between \mathbf{n}_k and \mathbf{n}_j , and r_k is a given *connection radius*. Fig. 1 shows the particular case in which the interacting neighbors of the generic node coincide with the nearest neighbors. We connect \mathbf{n}_k to each interacting neighbor \mathbf{n}_j through two elements working in parallel: a compressive masonry strut (or *bar*) $\mathbf{b}_i = \mathbf{n}_k - \mathbf{n}_j$, and a tensile FRP/FRCM element (or *string*) $\mathbf{s}_i = \mathbf{n}_k - \mathbf{n}_j$. We shall see in Sect. 3 that the minimal mass optimization of the background structure chooses which of such members (bar or string) is actually present between nodes \mathbf{n}_k and \mathbf{n}_j in the optimized configuration (i.e., which one of the above members actually carries a nonzero axial force in the minimal mass configuration, see also [30], Sect. 7). For future use, we let n_b and n_s denote the total number of bars and the total number of strings composing the background structure, respectively (with $n_b = n_s$ in the non-optimal configuration), and we set $n_x = n_b + n_s$.

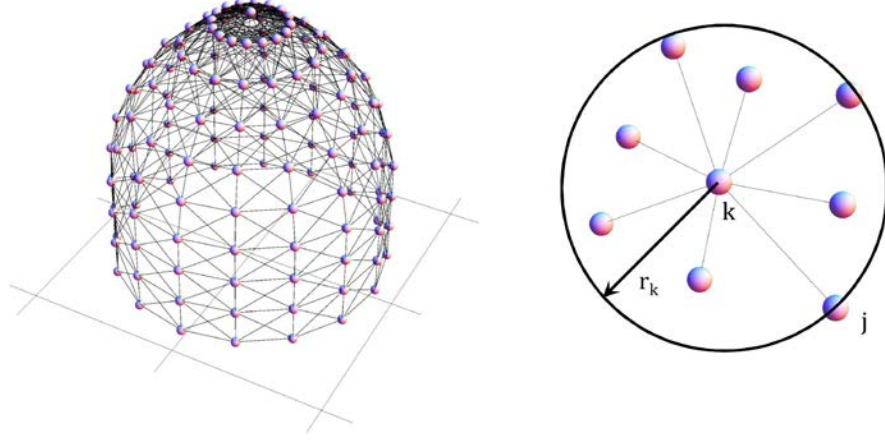


Figure 1: Background structure associated with a node set extracted from a dome (left) and nearest neighbors of a selected node (right).

We assume that the background structure is subjected to a number m of different loading conditions, and, with reference to the j -th condition, we let $\lambda_{b_i}^{(j)}$ denote the compressive force per unit length (force density) acting in the i -th bar, and let $\gamma_{s_i}^{(j)}$ denote the tensile force per unit length acting in the i -th string, both defined to be positive quantities. The static equilibrium equations of the nodes in correspondence of the current load condition can be written as follows

$$\mathbf{A}\mathbf{x}^{(j)} = \mathbf{w}^{(j)} \quad (2)$$

where \mathbf{A} is the $3n_n \times n_x$ *static matrix* of the structure, depending on the geometry and the connectivity of bars and strings (see [30]); $\mathbf{w}^{(j)}$ is *external load vector*, which stacks the $3n_n$ Cartesian components of the external forces acting on all nodes in the current loading condition; and $\mathbf{x}^{(j)}$ is the vector with n_x entries that collects the force densities in bars and strings in correspondence of the same loading condition, that is

$$\mathbf{x}^{(j)} = [\lambda_1^{(j)} \ \dots \ \lambda_{n_b}^{(j)} \ | \ \gamma_1^{(j)} \ \dots \ \gamma_{n_s}^{(j)}]^T \quad (3)$$

$$(4)$$

Let σ_{b_i} and σ_{s_i} respectively denote the compressive strength of the generic

bar and the tensile strength of the generic string of the background structure, which we hereafter assume behaving as elastic-perfectly-plastic members. Yielding constraints in bars and strings require that, for each loading condition, it results

$$\lambda_i^{(j)} b_i \leq \sigma_{b_i} A_{b_i}, \quad \gamma_i^{(j)} s_i \leq \sigma_{s_i} A_{s_i} \quad (5)$$

The masses of the generic bar and string of the background structure are computed as follows

$$m_{b_i} = Q_{b_i} A_{b_i} b_i, \quad m_{s_i} = Q_{s_i} A_{s_i} s_i, \quad (6)$$

where Q_{b_i} and Q_{s_i} denote the mass densities of such members.

3. Minimal Mass Design

Following [30], we formulate a *minimal mass design* of the background structure through the following linear program

$$\begin{aligned} & \text{minimize} && m = \mathbf{d}^T \mathbf{y} \\ & \mathbf{x}^{(j)}, \mathbf{y} && \begin{cases} \square \\ \square \end{cases} \mathbf{A} \mathbf{x}^{(j)} = \mathbf{w}^{(j)} \\ \text{subject to} &&& \begin{cases} \square \\ \square \end{cases} \mathbf{C} \mathbf{x}^{(j)} \leq \mathbf{D} \mathbf{y} \\ &&& \mathbf{x}^{(j)} \geq \mathbf{0}, \mathbf{y} \geq \mathbf{0} \end{aligned}, \quad (7)$$

where

$$\mathbf{y} = [A_{b_1} \cdots A_{b_{n_b}} \mid A_{s_1} \cdots A_{s_{n_s}}]^T \quad (8)$$

$$\mathbf{d}^T = [Q_{b_1} b_1 \cdots Q_{b_{n_b}} b_{n_b} \mid Q_{s_1} s_1 \cdots Q_{s_{n_s}} s_{n_s}] \quad (9)$$

$$\mathbf{C} = \begin{bmatrix} \text{diag}(\mathbf{b}_1, \cdots, \mathbf{b}_{n_b}) & \mathbf{0} \\ \mathbf{0} & \text{diag}(\mathbf{s}_1, \cdots, \mathbf{s}_{n_s}) \end{bmatrix} \quad (10)$$

$$\mathbf{D} = \begin{bmatrix} \text{diag}(\boldsymbol{\sigma}_{b_1}, \cdots, \boldsymbol{\sigma}_{b_{n_b}}) & \mathbf{0} \\ \mathbf{0} & \text{diag}(\boldsymbol{\sigma}_{s_1}, \cdots, \boldsymbol{\sigma}_{s_{n_s}}) \end{bmatrix} \quad (11)$$

Problem (7) returns an optimal configuration of the background structure, which consists of the set of all members (bars and strings) exhibiting nonzero

force density ($\lambda_i^{(j)}$ or $\gamma_i^{(j)}$) in at least one of the examined loading conditions. Such a configuration exhibits minimal mass among all the possible configurations of the background structure, under the equilibrium constraints (2) and the yielding constraints (5). It is worth noting that the mass of the background structure should not be confused with the self-weight of the masonry dome or vault under examination, which we agree to include in the external load vector $\mathbf{w}^{(j)}$ of the loading conditions accounting for gravity effects. The quantity subject to minimization in problem (7) should instead be regarded as the mass of an internal resisting mechanism of the structure. As we already observed, the latter is formed by a collection of masonry struts (bars), and a network of FRP/FRCM reinforcements loaded in tension (strings), which are able to carry axial forces that equilibrate the examined external loads without violations of the local yielding constraints.

4. Numerical Results

This section presents a parade of applicative examples of the optimization procedure formulated in Sect. 3, which deal with the FRP/FRCM reinforcement of a masonry dome (Sect. 4.1), and three different typologies of masonry vaults: a groin vault (or cross vault), a cloister vault (or domical vault) and a barrel vault (Sect. 4.2). Let $\{\mathbf{O}, \mathbf{x}, \mathbf{y}, \mathbf{z}\}$ be a Cartesian frame with the \mathbf{z} -axis oriented upward along the vertical direction. In all the examined examples, we consider the combined action of a vertical loading condition, corresponding to the action of the masonry self-weight, and four loading conditions combining the masonry self-weight with horizontal forces acting along the $+\mathbf{x}$, $-\mathbf{x}$, $+\mathbf{y}$, and $-\mathbf{y}$ directions, which are equal in magnitude to 35% of the vertical forces. The above horizontal forces mimic the effects of seismic excitations in two perpendicular directions of the examined structures, through a conventional, static approach to seismic actions on constructions (refer, e.g., to the European Standard [42]). We name *seismic loadings* the conditions that combine the masonry self weight with the above horizontal forces. We examine ‘Neapolitan’ tufo brick masonry, which is largely diffused in the area of Naples, with 15.0 kN/m^3 self-weight, and 13 MPa compressive strength σ_b (in all the bar elements). We assume a tensile strength σ_s equal to 376.13 MPa in all the string elements, which corresponds to an average value of the bond strengths of the FRP and FRCM reinforcements of masonry structures analyzed in [33, 34], respectively (we employed formula (5.6) of [39] to estimate such a strength). The examined background structures connect each

node to the nearest neighbors (Fig. 1) and are restrained by fixed hinge supports at the basis. We used the software Tensopt [43] to numerically solve problem (7).

4.1. The Dome of the church of Santa Maria di Monteverginella in Naples

We study the dome of the church of Santa Maria di Monteverginella in Naples, whose FRP-/FRCM-reinforcement has already been studied in [44] through a different, finite-element approach (refer to Fig. 2 for geometric details). We model the middle surface of the dome through a mesh with 145 nodes and 1504 connections (background structure in Fig 1). The optimal FRP/FRCM reinforcement patterns obtained through the procedure in Sect. 3 are shown in Figs. 3a-i.

Under vertical loading, the results in Figs. 3a-c highlight that the minimal mass FRP/FRCM reinforcements of the current structure are polar-symmetric and placed along parallel circles above the drum, with width increasing downward. Seismic loading in the \mathbf{x} direction instead combines parallel-circles' reinforcements with diagonal reinforcements placed over the portions of the dome parallel to the $\mathbf{x} - \mathbf{z}$ plane ($\pm\mathbf{y}$ edges, cf. Figs. 3d-f). In this case, the widths of the hoop reinforcements placed over the $+\mathbf{x}$ edge of the dome are considerably larger than the widths of the reinforcements placed over the $-\mathbf{x}$ edge.

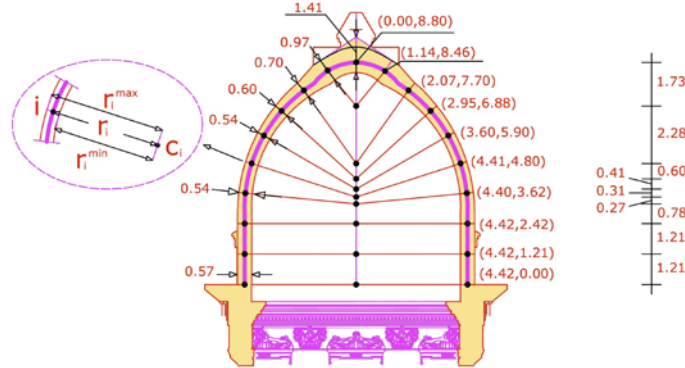


Figure 2: Cross-section of the dome of the church of Santa Maria di Monteverginella in Naples.

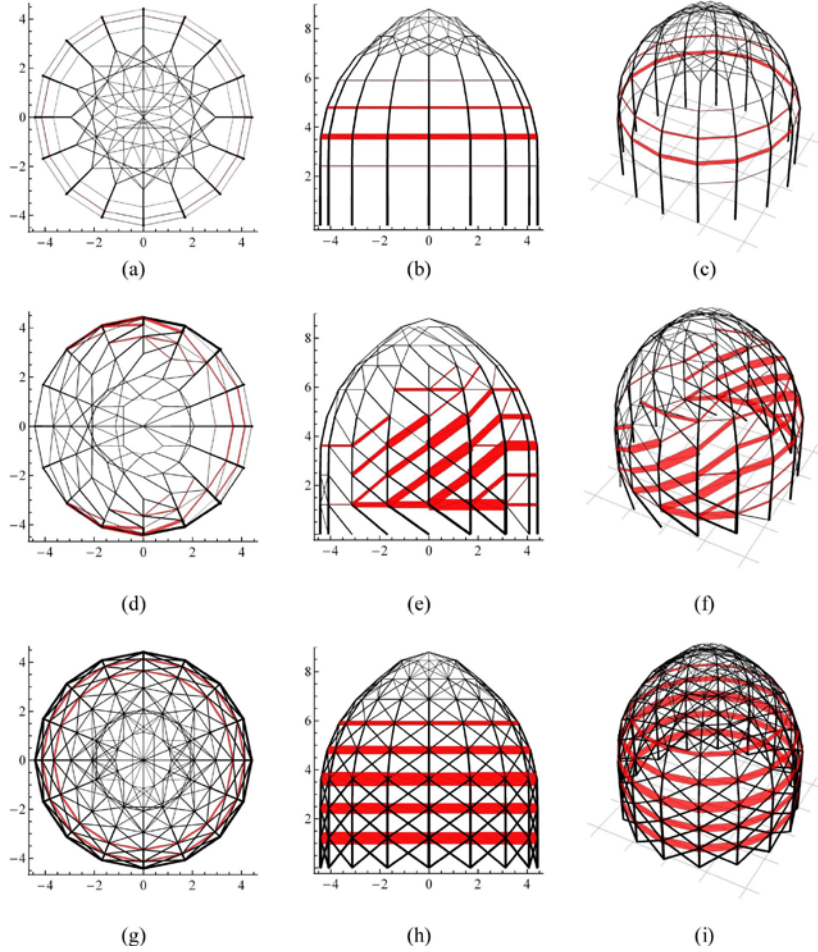


Figure 3: Top, side and 3D views of the optimal reinforcement patterns of a masonry dome with FRP/FRCM strips of thickness 0.34 mm (marked in red), under different loading conditions. (a)-(c): Vertical loading. (d)-(f): Seismic loading in the $+x$ -direction. (g)-(i): Combined vertical loading and seismic loading in two perpendicular directions.

The ‘combo’ loading condition combining vertical loading and seismic loading in two perpendicular directions returns polar-symmetric, parallel reinforcements with width increasing downward (Figs. 3g-i). It is worth noting that the FRP/FRCM reinforcements corresponding to seismic loading have markedly larger widths than those corresponding to vertical loading (compare Figs. 3a-c with Figs. 3g-i). The width of the top hoop reinforcements under vertical loading is about 100 mm (cf. Fig. 3a-c), while that of the central hoop reinforcements under combo seismic loading is 578 mm (cf. Fig.

3g-i). The compressed members of the internal resisting mechanism of the dome are mainly composed of meridian-shaped struts (Figs. 3a-c), which are associated with diagonal struts in presence of seismic loading (Figs. 3d-i). The results in Fig. 3 are in agreement with the frequent observations of ‘meridional’ (or ‘orange-slice’) crack patterns in unreinforced masonry domes (refer, e.g. to [41, 44] and references therein).

4.2. Groin, cloister and barrel vaults

Figs. 4, 5 and 6 show the minimal mass FRP/FRCM reinforcements that we obtained for a groin vault, a cloister vault and a barrel vault, respectively. The geometries of the examined vaults are illustrated in above figures, together with the corresponding background structures.

The background structure of the examined groin vault features 237 nodes and 1840 connections (cf. Figs. 4a-c). The minimal mass reinforcement pattern of such a vault consists of FRP/FRCM strips with thickness 0.17 mm on the web panels (width of the meridian strips near the crown under vertical loading: 340 mm; total width of the square reinforcing patch covering the crown under combo seismic loading: 3000 mm), and 200 mm \times 3.24 mm FRCM strips by the side of the groins at the corners (Fig. 4). The latter can also be replaced with pultruded FRP profiles with circular cross-section, 11.18 mm radius and 620.5 MPa tensile strength [45]. We observe that the above reinforcements prevent ‘hinging’ cracks departing from the crown and meridian cracks, in the case of vertical loading (Figs. 4d-f); and combined meridian cracks, cracks parallel to the groins, and the so-called ‘Sabouret’ cracks parallel to wall ribs, under vertical and seismic loading (Figs. 4g-l). The masonry strut network of the groin vault consist of four main arches at the intersection of the webs (ribs), which are completed by secondary meridian arches and diagonal struts over the webs.

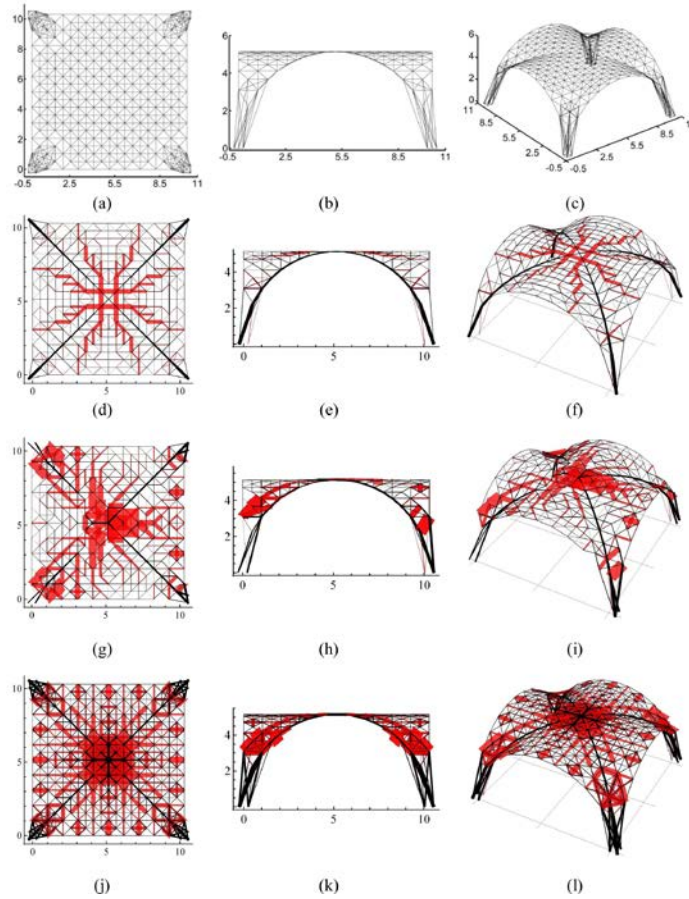


Figure 4: Top, side and 3D views of the optimal reinforcement patterns of a groin vault with FRP/FRCM strips of thickness 0.17 mm on the web panels, and 200 mm \times 3.24 mm FRCM strips or 11.18 mm radius pultruded FRP profiles at the corners (reinforcements marked in red). (a)-(c): Background structure. (d)-(f): Vertical loading. (g)-(i): Seismic loading in the $+x$ -direction. (j)-(l): Combined vertical loading and seismic loading in two perpendicular directions.

For the cloister vault we employed a background structure with 441 nodes and 4508 connections (see Figs. 5a-c). The optimal reinforcement of such a vault under vertical loading is mainly formed by parallel FRP/FRCM strips with 0.17 mm thickness and 82 mm maximum width near the crown (Figs. 5d-f). The above reinforcements are integrated with diagonal FRP/FRCM strips with about 140 mm maximum width near the intersections of the four vault segments, under combined vertical and seismic loading (Figs. 5g-l). The compressed network include couples of diagonal arches near the corners, parallel-line arches, and diagonal struts over the vault segments (Figs. 5d-l).

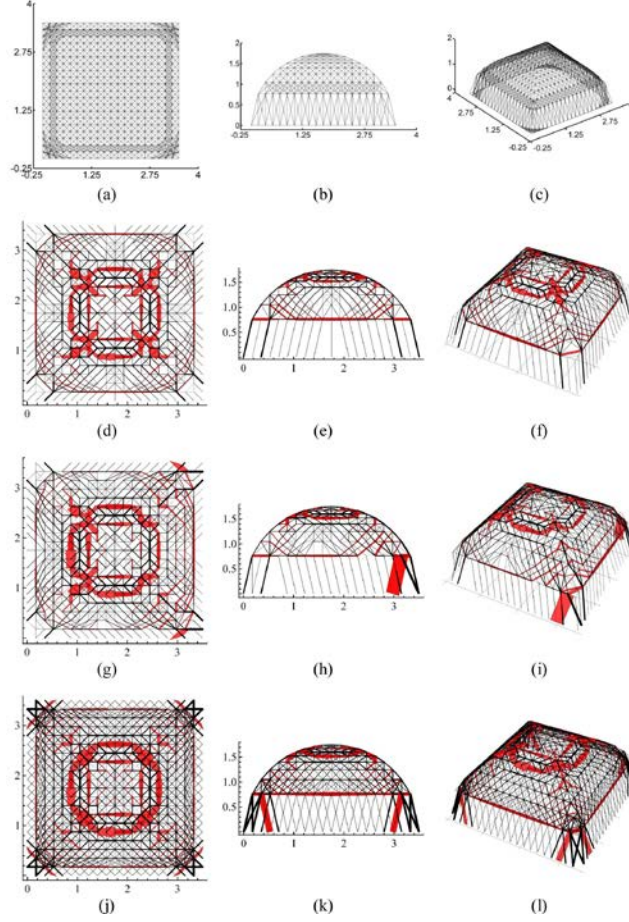


Figure 5: Top, side and 3D views of the optimal reinforcement patterns of a cloister vault with FRP/FRCM strips of thickness 0.17 mm (marked in red), under different loading conditions. The widths of the FRP/FRCM reinforcements are magnified by a factor 2 for visual clarity. (a)-(c): Background structure. (d)-(f): Vertical loading. (g)-(i): Seismic loading in the $+x$ -direction. (j)-(l): Combined vertical loading and seismic loading in two perpendicular directions.

In the case of the barrel vault, we focus our attention on the combined action of vertical loading, seismic loading in the $+x$ direction (Figs. 6a-c), and seismic loading in two orthogonal directions (Figs. 6d-f), neglecting simple vertical loading. The above loading conditions induce a three-dimensional state of stress in the barrel vault, while pure vertical loading allows for discretizing the structure in a series of independent parallel arches (refer, e.g., to [41], Sect. 4.1). The background structure of the current vault is composed of 231 nodes and 1660 connections (Fig. 6). The resisting mechanism of the barrel vault under seismic loading includes transverse compressed arches, lon-

itudinal FRP/FRCM strips with 0.17 mm thickness, and diagonal struts, as shown in Figs. 6d-f. The FRP/FRCM reinforcements feature rather small width in the present case (minimum width: 0.1 mm; maximum width: 4 mm), and have been magnified by a factor 10 in Fig. 6 for visual clarity.

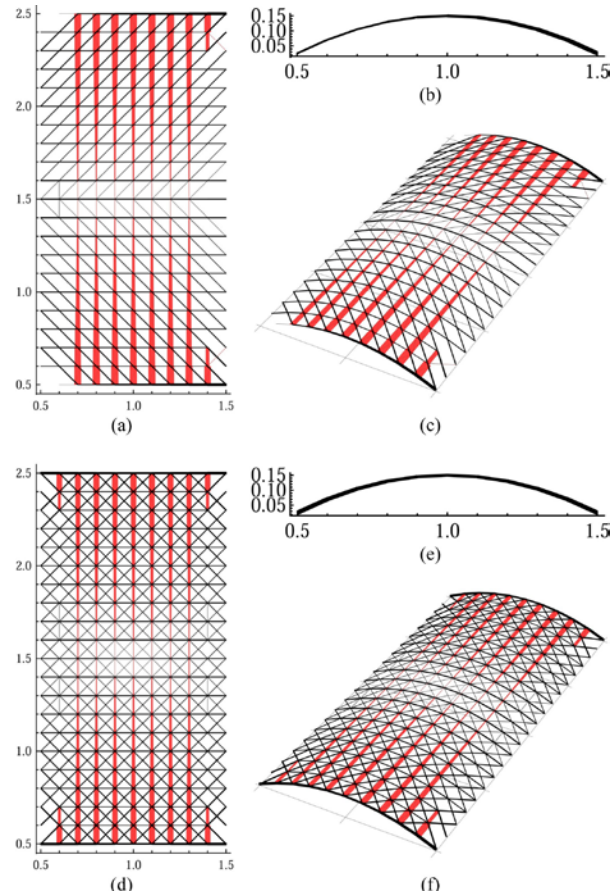


Figure 6: Top, side and 3D views of the optimal reinforcement patterns of a barrel vault with FRP/FRCM strips of thickness 0.17 mm (marked in red). The widths of the FRP/FRCM reinforcements are magnified by a factor 10 for visual clarity. (a)-(c): Seismic loading in the $+x$ -direction. (d)-(f): Combined vertical loading and seismic loading in two perpendicular directions.

5. Concluding remarks

We have presented a minimal mass approach to the search for internal resisting mechanisms of masonry domes and vaults composed of compressed

masonry struts and tensile FRP/FRCM reinforcements. Such mechanisms can be regarded as tensegrity models of the examined structures, in line with available technical standard for the FRP reinforcement of masonry structures [39]. The existence of internal resisting mechanisms for given yielding constraints ensures that the reinforced structure is safe under the examined loading conditions, according to the safe theorem of the limit analysis of elastic-plastic bodies [40]. Several numerical examples have highlighted the potential of the proposed approach in designing non-invasive FRP/FRCM reinforcements of masonry vaults and domes, which may ensure sufficient ‘cracking-adaptation’ capacity of the reinforced structure.

Future directions of the present study will be aimed at formulating tensegrity models of FRP/FRCM reinforced planar masonry structures (e.g., masonry walls), and three-dimensional assemblies of domes, vaults and supporting structures (including walls, piers, flying buttresses; drums; etc.). Additional extension of the present research will deal with discrete-to-continuum approaches to tensegrity membranes [6], and 3D tensegrity networks.

Acknowledgments

The authors wish to acknowledge the great support received by Ada Amendola and Mariella De Piano (Department of Civil Engineering, University of Salerno, Italy) during the course of the present work.

6. References

- [1] Zhu HP, Zhou ZY, Yang RY, Yu AB. Discrete particle simulation of particulate systems: A review of mayor applications and findings. *Chem Eng Sci* 2008;63:5728–5770.
- [2] Liu B, Huang Y, Jiang H, Qu S, Hwang KC. The atomic-scale finite element method. *Comput Methods Appl Mech Engrg* 2004;193:1849–1864.
- [3] Badia S, Parks M, Bochev P, Gunzburger M, Lehoucq R. On atomistic-to-continuum coupling by blending. *Multiscale Model Sim* 2008;7(1):381–406.
- [4] Belytschko T, Xiao SP. Coupling methods for continuum model with molecular model. *Int J Multiscale Com* 2003;1(1):115–126.
- [5] Shenoy VB, Miller R, Tadmor EB, Rodney D, Phillips R, Ortiz M. An adaptive finite element approach to atomic-scale mechanics-the quasicontinuum method. *J Mech Phys Solids* 1999;47:611–642.

- [6] Schmidt B, Fraternali F. Universal formulae for the limiting elastic energy of membrane networks. *J Mech Phys Solids* 2012;60:172–180.
- [7] Fraternali F. Free Discontinuity Finite Element Models in Two-Dimensions for In-Plane Crack Problems. *Theor Appl Fract Mec* 2007;47:274–282.
- [8] Fraternali F, Angelillo M, Fortunato A. A lumped stress method for plane elastic problems and the discrete-continuum approximation. *Int J Solids Struct* 2002;39:6211–6240.
- [9] Davini C, Pitacco I. Relaxed notions of curvature and a lumped strain method for elastic plates. *SIAM J Numer Anal* 2000;35:677–691.
- [10] Fraternali F, Carpentieri G. On the Correspondence Between 2D Force Networks and Polyhedral Stress Functions. *International Journal of Space Structures* 2014;29(3):145–159.
- [11] O’Dwyer D. Funicular analysis of masonry vaults. *Comput Struct* 1999;73:187–197.
- [12] Block P, Ochsendorf J. Thrust Network Analysis: A new methodology for three-dimensional equilibrium. *IASS J* 2007;48(3):167–173.
- [13] De Goes F, Alliez P, Owhadi H, Desbrun M. On the equilibrium of simplicial masonry structures. *ACM Transactions on Graphics* 2013;32(4):93.
- [14] Block P. Thrust Network Analysis: Exploring Three-dimensional equilibrium. PhD dissertation, Massachusetts Institute of Technology, Cambridge, USA, 2009.
- [15] Fraternali F. A thrust network approach to the equilibrium problem of unreinforced masonry vaults via polyhedral stress functions. *Mech Res Commun* 2010;37:198–204.
- [16] Fraternali F. A mixed lumped stress–displacement approach to the elastic problem of masonry walls. *Mech Res Commun* 2011;38:176–180.
- [17] Fraternali F, Blegesen M, Amendola A, Daraio C. Multiscale mass-spring models of carbon nanotube foams. *J Mech Phys Solid* 2010;59(1):89–102.
- [18] Ngo D, Fraternali F, Daraio C. Highly nonlinear solitary wave propagation in T-shaped granular crystals with variable branch angles. *Phys Rev E* 2012;85:036602-1-10.

- [19] Schlaich J, Schäfer K, Jennewein M. Toward a Consistent Design of Structural Concrete. *J Prestr Concrete I (PCIJ)* 1987;32:74–150.
- [20] Fraternali F. Error estimates for a lumped stress method for plane elastic problems. *Mech Adv Matl Struct* 2007;14(4):309–320.
- [21] Blesgen T, Fraternali F, Raney JR, Amendola A, Daraio C. Continuum limits of bistable spring models of carbon nanotube arrays accounting for material damage. *Mech Res Commun* 2012;45:58–63.
- [22] Davini C, Paroni R. Generalized hessian and external approximations in variational problems of second order. *J Elast* 2003;70:149–174.
- [23] Ingber DE. The architecture of life. *Sci Am* 1998;278(1):48–57.
- [24] Fraternali F, Senatore L, Daraio C. Solitary waves on tensegrity lattices. *J Mech Phys Solids* 2012;60:1137–1144.
- [25] Fraternali F, Carpentieri G, Amendola A, Skelton RE, Nesterenko VF. Multiscale tunability of solitary wave dynamics in tensegrity metamaterials. *Appl Phys Lett* 2014;105:201903.
- [26] Amendola A, Fraternali F, Carpentieri G, de Oliveira M, Skelton RE. Experimental investigation of the softening-hardening response of tensegrity prisms under compressive loading. *Compos Struct* 2014;117:234–243.
- [27] Skelton RE, de Oliveira MC. Optimal complexity of deployable compressive structures. *J Franklin I* 2010;347:228–256.
- [28] Skelton RE, de Oliveira MC. Optimal tensegrity structures in bending: the discrete Michell truss. *J Franklin I* 2010;347:257–283.
- [29] Skelton RE, de Oliveira MC. *Tensegrity Systems*. Springer, 2010.
- [30] Nagase K, Skelton RE. Minimal mass tensegrity structures, *Journal of the International Association for Shell and Spatial Structures* 2014;55(1):37–48.
- [31] Skelton RE, Fraternali F, Carpentieri G, Micheletti A. Minimum mass design of tensegrity bridges with parametric architecture and multiscale complexity. *Mech Res Commun* 2014;58:124–132.
- [32] Carpentieri G, Modano M, Fabbrocino F, Fraternali F. Optimal design and dynamics of truss bridges. *CompDyn* 2015, 25-27 May 2015.

- [33] Mazzotti C, Ferracuti B, Bellini A. Experimental bond tests on masonry panels strengthened by FRP. *Compos Part B-Eng* 2015; 80:223–237.
- [34] Carozzi FG, Poggi C. Mechanical properties and debonding strength of Fabric Reinforced Cementitious Matrix (FRCM) systems for masonry strengthening. *Compos Part B-Eng* 2015; 70:215–230.
- [35] Milani G, Simoni M, Tralli A. Advanced numerical models for the analysis of masonry groin vaults: A case-study in Italy. *Eng Struct* 2014;76:339–358.
- [36] Baratta A, Corbi O. An approach to the positioning of FRP provisions in vaulted masonry structures. *Compos Part B-Eng* 2013;53:334–341.
- [37] Baratta A, Corbi O. Closed-form solutions for FRP strengthening of masonry vaults. *Comput Struct* 2015;147:244–249.
- [38] Angelillo M, Babilio E, Cardamone L, Fortunato A, Lippiello M. Some remarks on the retrofitting of masonry structures with composite materials. *Compos Part B-Eng* 2014;61:11–16.
- [39] Italian National Research Council (CNR), Guide for the Design and Construction of Externally Bonded FRP Systems for Strengthening Existing Structures - Materials, RC and PC structures, masonry structures. CNR-DT 200/2013 - R1, Rome, Italy, 2013.
- [40] Koiter WT. General Theorems for Elastic-Plastic Solids, in: *Progress in Solid Mechanics*. Sneddon J.N., Hill R. (eds.), North-Holland, Amsterdam, 1:165-221, 1960.
- [41] Heyman J. *The Stone Skeleton*. Cambridge University Press, Cambridge, 1995.
- [42] European Committee for Standardization. Eurocode 8: Design of structures for earthquake resistance. Part 1: General rules, seismic actions and rules for buildings. EN 1998-1:2004, Brussels, Belgium, 2014.
- [43] Fraternali F, Carpentieri G. Tensopt, Computer software, 2014. Retrieved from <http://www.fernandofraternaliresearch.com/downloads.asp?pg=9>.
- [44] Fabbrocino F, Farina I, Berardi VP, Ferreira AJM, Fraternali F. On the Thrust Surface of Unreinforced and FRP-/FRCM-Reinforced Masonry Domes, *Compos Part B-Eng* 2015; In Press.
- [45] Bedford Reinforced Plastics, Design Manual, Revise 4/12, Bedford, PA 15522-7401 USA; [accessed online 2015 Aug 06]. <http://bedfordreinforced.com/>.